NON-INDUCTIVE CURRENT DRIVE WITH SUPRATHERMAL IONS AND ELECTRONS IN REACTOR-GRADE TOKAMAK PLASMAS: A COMPARISON

IPP 4/242 May 1990

D. Eckhartt

MAX-PLANCK-INSTITUT FÜR PLASMAPHYSIK

8046 GARCHING BEI MÜNCHEN

MAX-PLANCK-INSTITUT FÜR PLASMAPHYSIK
GARCHING BEI MÜNCHEN

NON-INDUCTIVE CURRENT DRIVE WITH SUPRATHERMAL IONS AND ELECTRONS IN REACTOR-GRADE TOKAMAK PLASMAS: A COMPARISON

IPP 4/242 May 1990

D. Eckhartt

Die nachstehende Arbeit wurde im Rahmen des Vertrages zwischen dem Max-Planck-Institut für Plasmaphysik und der Europäischen Atomgemeinschaft über die Zusammenarbeit auf dem Gebiete der Plasmaphysik durchgeführt.

Non-inductive Current Drive with Suprathermal Ions and Electrons in Reactor-Grade Tokamak Plasmas: A Comparison

D. Eckhartt

May 1990

I. Introduction

It is now widely accepted that a prospective fusion reactor will be a tokamak configuration and operate in steady-state. Two main requirements must be met in order to have this toroidal magnetic confinement scheme running in a truely stationary mode:

- the ion species composition in the plasma and its radial distribution must be controlled
- the toroidal current through the plasma must be sustained by non-inductive means

The first condition implies, for example, the supply of fuel ions to the plasma centre at adequate rates, as well as the presence of non-fuel ions/atoms at the plasma edge to radiate away part of the outward-streaming heat power. Of paramount importance is the removal of helium "ash" and other impurities from the central parts of a burning DT-plasma. Otherwise this plasma region will be depleted from fuel ions, and the fusion power production slows down. No convincing scheme has yet been found (let alone tested) for the controlled ash and impurity removal from the central plasma regions. If this problem cannot be solved without impairing plasma confinement and temperature distribution, the burn phase must be interrupted periodically in order to clean and re-fill the reactor.

With regard to the second requirement: completely non-inductive current-drive with fast ions or electrons has already been demonstrated experimentally. Some examples will be discussed below in more detail. The fast ions were created by injecting neutral beams of high-energy atoms /1/, the suprathermal electrons by Landau-resonance of bulk plasma electrons with lower hybrid waves travelling along the magnetic field lines /2,3,4/,

they were launched as slow waves /5/ at the plasma edge. The power to sustain the population of suprathermal particles against thermalizing collisions with the background plasma particles is drawn from the energy of the "drivers", neutral beams or waves. In all experiments conducted up to now the background plasmas were well below reactor relevance: densities and temperatures were lower by about one order of magnitude each. Hence one must rely on current drive theories /6,7/ to predict the performance in future reactor-grade plasmas. In the following Report we shall compare such predictions on current drive by fast ions and electrons and discuss the consequences of the extrapolations. In either case large amounts of driver power must be deposited to sustain the toroidal current continuously. Whether such a steady state is really desirable depends on our ability to control the plasma species composition - as mentioned above.

A central quantity in theoretical and practical considerations on current drive is its efficiency γ. It relates the total driven current I_d to the power P_{abs} absorbed by the plasma from the driver and required to sustain the current I_d. This power is normalized to the unit of toroidal length R_o, and to the average electron density $\bar{n}_e$. Thus:

$$\gamma = \frac{I_d}{P_{abs}/R_o \cdot \bar{n}_e} \quad [A, W, m, 10^{20} \cdot m^{-3}] \qquad (1)$$

The number values of γ allow to compare the results of the two current drive schemes that were obtained in various machines. It turns out that their theoretically predicted γ-values in reactor plasmas lie quite close to each other - a surprising (but probably fortuitous) result if one considers how different the mechanisms are which generate the suprathermal populations in the two cases.

Another quantity of interest is the ratio between current and power, the figure of merit η. Later we shall use a local figure of merit, defined by:

$$\eta_f = \frac{j_f}{p_f} \quad [A/cm^2, Watt/cm^3] \qquad (2)$$

which relates the current density j_f of the suprathermal particles to the power density p_f lost by these fast particles during their collisional

slowing-down and supplied by the driver in steady-state. It is this quantity η_f which can be made available by theory under certain idealizing conditions such as a homogeneous background plasma in a straight magnetic field. The transition to "real" systems with spatially variable parameters must then be accomplished with the help of additional assumptions.

II. A Simplified Picture of Current Drive and its Figure of Merit

Let us consider a group of fast charged particles which move through a thermal background plasma along the lines of force of a straight magnetic field. The symbols m_f, q_f, v_f, n_f, denote, respectively, their mass, electric charge, velocity, and density. They loose kinetic energy in collisions with the background thermal plasma. The rate of this energy transfer to the plasma is determined by $(1/t_s)$ where t_s is the slowing-down time of an average fast particle.

The current density carried by the fast particles is given by:

$$j_f = q_f \cdot v_f \cdot n_f \qquad (3)$$

whereas the power density transferred by collisions to the background plasma can be written as:

$$p_f = (n_f/t_s) \cdot 1/2 \cdot m_f v_f^2 \qquad (4)$$

The ratio of the two quantities defines the local figure of merit η_f:

$$\eta_f = 2 \cdot q_f/(m_f \cdot v_f) \cdot t_s \qquad (5)$$

which is independent of the fast particle density.

Let us now compare a beam of fast suprathermal electrons ($m_f = m_e$, $q_f = e$, $v_f = v_{be}$, $1/2\, m_e \cdot v_{be}^2 = E_{be}$) with a beam of fast ions ($m_f = A_b \cdot m_p$, $q_f = Z_b \cdot e$, $v_f = v_{bi}$) whose velocity v_{bi} is smaller than the thermal speed v_{te} of the background plasma electrons but larger than the ion thermal speed v_{ti}. In this case the slowing-down process occurs primarily via collisions with background electrons. Hence the respective slowing down times are given by the electron collision times which - in turn - are determined by the velocity of the faster of the two colliding particles, thus:

$$t_{si} \propto v_{te}^3/n_e \qquad t_{se} \propto v_{be}^3/n_e \tag{6}$$

By combining eqs. (5) and (6) one obtains:

$$n_e \cdot \eta_{fi} \propto (v_{te}/v_{bi}) \cdot T_e \tag{7a}$$

$$n_e \cdot \eta_{fe} \propto E_{be} \tag{7b}$$

It is clear from this simple derivation that fast ion current drive can become more efficient, compared to that of suprathermal electrons, when the electron temperature is raised. On the other hand, E_{be} is given by the parallel phase velocity of the wave which, in turn, is determined by the topology of the launching structure and hence does not offer many possibilities for further optimization compared to present-day experiments. This conclusion remains valid even if one takes into account that the fast ion current is partially compensated by a counter current carried by background plasma electrons. This electron screening effect depends on the effective plasma charge and on the local aspect ratio of the plasma toroid but not on bulk plasma density and temperature /7/.

By inserting exact expressions for the the slowing-down times of fast ions /8/ and of fast electrons /9/ in eq.(5) we can get more precise results within the frame of our simple model. We have:

$$t_{si} = (\tau_{se}/3) \cdot \ln\left[1+(E_{bi}/E_c)^{3/2}\right] \tag{8}$$

Here τ_{se} is the electron collision time /10/ which reads in practical units (the Coulomb logarithm is taken to be $\ln\Lambda_e = 17$):

$$\tau_{se} = (0{,}37s)\,\frac{A_b}{Z_b^2}\left(\frac{T_e}{10\ \mathrm{keV}}\right)^{3/2}\left(\frac{10^{14}\mathrm{cm}^{-3}}{n_e}\right) \tag{9}$$

and E_c is the so-called critical energy, $E_c \propto T_e$, where equal amounts of energy are transferred from the fast ion to the plasma electrons and ions during its slowing-down process /10/. With t_{si} from eq.(8) we can rewrite eq.(7a):

$$n_e \cdot n_{fi} \propto T_e \cdot (v_{te}/v_{bi}) \cdot \ln[1+C \cdot (v_{bi}/v_{te})^3] \qquad (7c)$$

(where C is a numerical constant). It is now clearly evident that T_e is the leading variable in eq.(7c) since the other two multipliers form a function of (v_{bi}/v_{te}) which passes through a broad maximum. The fast electron slowing-down time can be expressed in terms of τ_{se}:

$$t_{se} = \tau_{se} \cdot (4\ Z_b^2/9\ \pi^{1/2})(m_e/A_b \cdot m_p)(E_{be}/T_e)^{3/2} \qquad (10)$$

which, in fact, is independent of T_e since τ_{se} grows as $T_e^{3/2}$, c.f. eq.(9).

III. Short Survey of Experimental Results

Non-inductive current drive with uni-directional injection of lower hybrid waves or neutral beams has been studied in a number of tokamak experiments. Here we restrict ourselves to such cases where a stationary state, free of inductive effects, could be established. This was done by setting the primary current in the ohmic heating transformer to a constant value, or by clamping the plasma current and driving the loop voltage to zero. In both cases this state must be maintained for such a long time that the plasma current and its internal distribution can relax to an equilibrium state ($dl_i/dt = 0$, l_i = internal inductance). In addition, the pressure-driven boot-strap currents must be properly accounted for - preferably their contribution to the total current should be negligibly small. For neutral beam current drive these conditions were only fulfilled in the DIII-D experiment where a plasma with H-mode quality was entirely sustained by high-power neutral beam injection /1/. Some relevant data are listed in the Table on the following page, together with results of three lower hybrid slow wave experiments /2,3,4/. The largest current (I_p = 2 MA) and the highest efficiency (γ = 0,265) are reported from the JT-60

Experiment		JT-60 [2]	ASDEX [4]	PLT [3]	DIII-D [1]
R_o	[m]	3,03	1,68	1,32	1,69
I_p	[MA]	1	0,45	0,52	0,34
P_{abs}	[MW]	1,25	1,02	0,52	10
$\bar{n}_e$	[$10^{13}m^{-3}$]	0,9...1,25	1,52	1	2
γ_{exp}		0,2...0,29	0,15	0,132 0,14[1])	0,012
γ_{th}			0,15	0,2[2])	0,029[3])
$T_e(0)$	[keV]		6,44	2 ... 6	2
$\bar{T}_e$	[keV]	1 ... 2	1,46		1,6[4])
Z_{eff}		3 ... 6	6,5	3 ... 4	2[5])
τ_E	[ms]	150	47	15[6])	24
t_s[7])	[ms]	32 ... 23	5,5	45	95
β_p		0,3			3,5
f	[GHz]	2	2,45	2,45	-
$N_{\parallel}$		$1,6^{+0,9}_{-0,6}$	2,2 ± 0,4	1,5 ± 0,45	-
E_{be} at $N_{\parallel}^{max}$	[keV]	150	65	200	-
E_{bi}	[keV]	-	-	-	75

[1]) value corrected for residul inductive effects

[2]) γ_{exp} divided by 0,7 (see text at bottom of page 5)

[3]) calculated by assuming constant (mean) values of density and temperature

[4]) $T_e(0)$ divided by a "profile factor" of 1,25

[5]) assuming a pure background helium plasma

[6]) private communication by Dr. T.K.Chu from Princeton University

[7]) calculated from eqs.(8) and (10).

tokamak*). The efficiency even reached 0,3 when balanced neutral beam injection was added. The bootstrap current was relatively small /11/. In PLT the influence of the shape of the lower hybrid wave spectrum on the figure of merit was studied: the fastest wave spectrum which could be generated, was optimum for current drive /3/. The measured efficiencies were also compared with values from an idealized theory in a relativistic plasma and for a very narrow wave spectrum /12/ - assuming constant plasma temperature and density in the plasma. For such a comparison the experimental data like wave spectra and plasma profiles must be normalized as mentioned in Ref. /3/. In general the measured efficiencies were found to be 60 to 80 % of the theoretical numbers. Better agreement between experiment and (non-relativistic) theory /12/ was found in ASDEX after taking proper account of the emitted wave power spectrum. The data /4/ shown in the Table are such an example. Box-type plasma profiles were also used to calculate γ for the beam current drive in DIII-D with the formalism developed in the following Chapter (c.f. eq.(17)) yielding $\gamma_{exp}/\gamma_{th} = 0,35$.

The experiments listed in the Table were all made with similar but rather low average electron densities ($\bar{n}_e = 1...2 \cdot 10^{13}$ cm^{-3}) and temperatures ($\bar{T}_e = 1...2$ keV). For these bulk plasma parameters neutral beam current drive is found 10 times less efficient than lower hybrid current drive. In general, the measured efficiencies are smaller than those derived from theory. But they get closer when the energy confinement times become longer in relation to the fast particle slowing-down times /1/. Such a trend was predicted by theory when fast particle life times are included /13,14/ which, in present experiments, can be taken as approximately equal to the bulk electron energy confinement times /13/. It could also explain why in JT-60, where $\tau_E > t_s$, the highest efficiencies were observed.

In the simplified non-relativistic plasma model of lower hybrid current drive the efficiency depends only on Z_{eff} and on the wave power spectrum but not on temperature. Over the range of temperature present in PLT one might have expected efficiency variations of approximately 10 % upon

---

*) in this machine the H-mode could be attained during lower hybrid current drive in limiter discharges /11/.

considering relativistic effects /3/. But such small changes were completely masked by other effects, and it was not possible to vary T_e independently of other important parameters such as plasma current /3/ which determines the energy confinement time. In ASDEX no temperature dependence was found /15/. It is only in JT-60 where a linear increase with electron temperature of the current drive efficiency has been reported /2, 16/. But the published experimental data do not support such a claim: in Ref./17/ there are data points for which the efficiency stays constant when T_e is increased from 1 to 2 keV, as well as other ones for which the efficiency changes from 0,2 to 0,3 at constant T_e. In the next Chapter we shall return to this temperature dependence when we take a closer look at the theoretical predictions on lower hybrid current drive in relativistic plasmas.

Let us consider experimental evidence for the existence of a suprathermal ion or electron population. Such measurements could prove the ideas on neutral beam or wave absorption, and on the collisional slowing down processes. The energy distribution of fast ions was measured using charge exchange spectroscopy, and good agreement with theory was found /18, 19/. The ion velocity distribution of the background plasma ions is modified during injection as shown schematically in Fig. 1a). Recently classical test-particle deceleration has been proved by observing the neutron emission from fusion reactions between injected fast atoms/ions and the deuterium atoms in the background plasma /21/. The suprathermal electron velocity distribution during lower hybrid current drive can be inferred from the bremsstrahlung emitted by these fast electrons. It requires spatially resolved hard X-ray spectra to be taken as function of photon energy and emission angle /22/. This is an "indirect" measurement since the photon energy distribution is not the electron energy distribution. One must assume a model for the electron distribution in velocity and configuration space and determine its consistency with the measured data. In general, agreement could be found with the theoretically predicted parallel velocity distribution /23/ of Fig. 1b) which features the plateau being created by quasi-linear Landau damping of lower hybrid waves with parallel phase velocities v_p in the resonant region $v_p/v_{te} = w_1 \ldots w_2$.

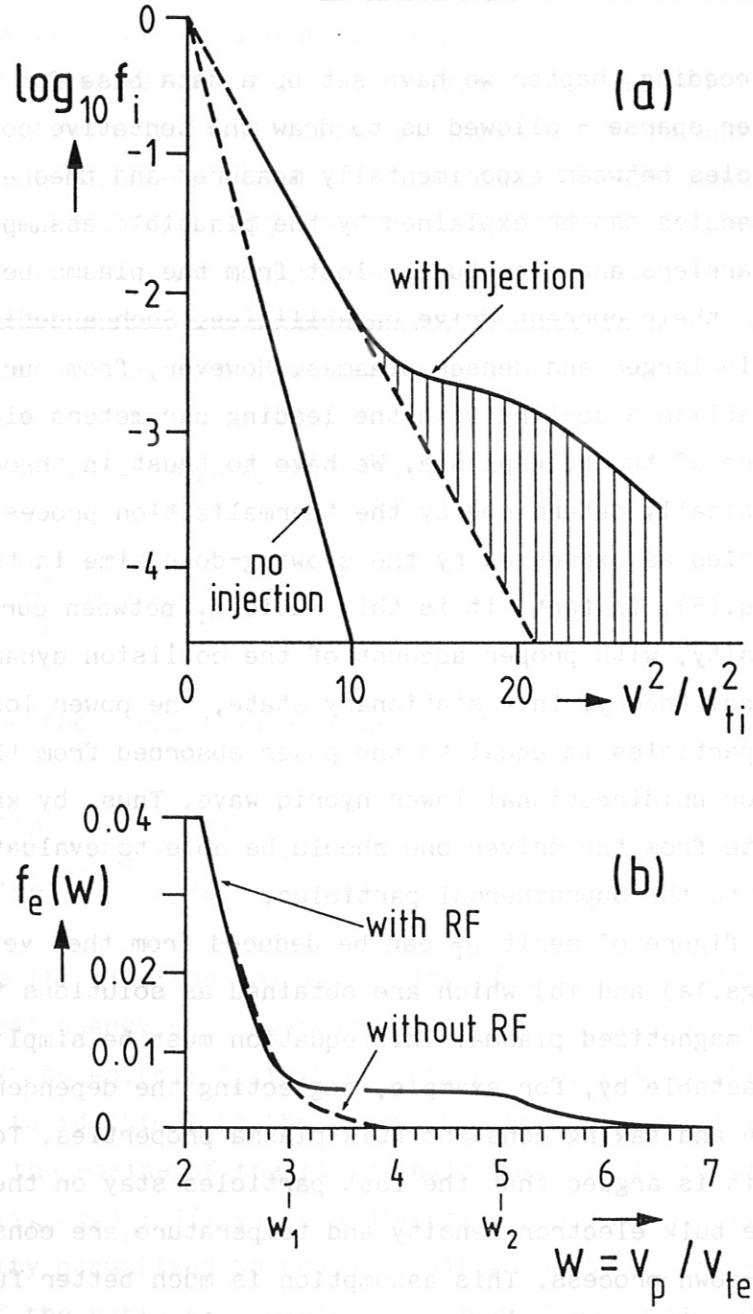

Fig. 1a): The calculated ion energy distribution function without and with injection of fast ions having $v_{bi}^2/v_{ti}^2 = 100$ (from Ref./20/).

Fig. 1b): Parallel electron velocity distribution following injection of lower hybrid slow waves with phase velocities v_p, normalized to the thermal velocity v_{te}, between $w_1 = 3$ and $w_2 = 5$. Note that the maximum value f_e at $w = 0$ is 0,38 (from Ref./6/).

IV. A Glimpse at Current Drive Theories

In the preceding Chapter we have set up a data base for current drive which - however sparse - allowed us to draw the tentative conclusion that the discrepancies between experimentally measured and theoretically expected efficiencies can be explained by the plausible assumption that the fast charge carriers are prematurely lost from the plasma before having fully used up their current drive capabilities. Such a deficiency will no longer exist in larger and denser plasmas. However, from our date base we could not establish a scaling with the leading parameters electron density and temperature of the bulk plasma. We have to trust in theory that this scaling is basically determined by the thermalization process of the suprathermal particles as expressed by the slowing-down time in the local figure of merit of eq.(5). In fact, it is this ratio η_f between current density and power density, with proper account of the collision dynamics, which we hope to get from theory. In a stationary state, the power lost by the suprathermal particles is equal to the power absorbed from the driver - neutral beam or unidirectional lower hybrid wave. Thus, by knowing the absorption rate from the driver one should be able to evaluate the current density owing to the suprathermal particles.

The local figure of merit η_f can be deduced from the velocity distributions of Figs.1a) and 1b) which are obtained as solutions to the kinetic equation of a magnetized plasma. This equation must be simplified in order to make it tractable by, for example, neglecting the dependence on configuration space and taking constant bulk plasma properties. To justify this idealization it is argued that the fast particles stay on the same flux surface, where bulk electron density and temperature are constant, during their slowing-down process. This assumption is much better fulfilled for electrons than for ions (of comparable energies) since the fast particle excursions from the flux surface where they have been born, are of the order of the radius of gyration. Thus the simplified kinetic equation describes the velocity space evolution of a fast particle population in a homogeneous plasma. In order to obtain the steady-state velocity distribution we must specify sources and sinks of the fast particle numbers and velocities/energies. Since they are relatively few in number their sink is simply the "sea" of background thermal particles. The source term is

readily quantified in the case of current drive with a mono-energetic neutral beam which we shall consider first.

The fast ions are born through ionization of the neutral beam particles, and their initial velocity components along and across the magnetic field lines are defined by the beam direction. Hence the fast particle source can be easily modelled which allows an analytic steady-state solution to the ion kinetic equation, yielding for the local values of ion current density and power density, resp., in a homogeneous fully ionized plasma embedded in a straight magnetic field /7/:

$$j_{fi} = e \cdot Z_b \cdot S_o \cdot \xi_o \cdot \tau_{se}/v_c \cdot v_b^2 \cdot J(x,y) \qquad (11)$$

$$p_{fi} = \frac{A_b \cdot m_p \cdot v_b^2}{2} \cdot S_o \qquad (12)$$

and hence for the local figure of merit /24/:

$$\eta_{fi} = \frac{2e \cdot Z_b}{A_b \cdot m_p} \cdot \xi_o \cdot \frac{\tau_{se}}{v_c} \cdot J(x,y) \qquad (13)$$

Here: τ_{se} is the electron collision time of eq. (9); v_c is defined by the critical energy $E_c = A_b \cdot m_p \cdot v_c^2/2 \propto T_e$ which was already introduced in context to eq.(8); S_o is the birth rate of fast particles (im cm^{-3} s^{-1}) which is identical to the (negative) neutral beam loss rate; ξ_o is the cosine of the pitch angle when the fast ions are born: $\xi_o = (v_{b\parallel}/v_b)_o$; J(x,y) is a dimensionless function of the beam velocity normalized to the critical velocity $v_{bo}/v_c = (E_b/E_c)^{1/2} = x$, and of the ratio $4 \cdot Z_{eff}/5A_b = y$, where Z_{eff} is the effective charge of the background plasma.

The deposition factor J has a characteristic dependence on x, i.e. on the bulk electron temperature for a given beam energy: for relevant values of y one finds a broad maximum when $x^2 = E_b/E_c$ is larger than 2. This implies that the figure of merit eq.(13) scales as $\tau_{se}/v_c \propto T_e/n_e$, as was already suggested in the context to eq.(7c).

By means of collisions the unidirectionally streaming fast ions transfer momentum to the background plasma electrons. These respond by setting up an electric current in the opposite direction which partially cancels the primary ion current. This electron counter current is taken into account by using a multiplier F_e to the fast ion current density. Hence the (net) figure of merit is given by:

$$\eta_i = \eta_{fi} \cdot F_e \qquad (14)$$

For a plasma in a tokamak magnetic field configuration "neo-classical" effects have to be considered for both fast ions and co-streaming bulk electrons. A correction factor F_{nc} of order unity is applied to the ion current density in eq.(11), and hence to the figure of merit eq.(13). F_{nc} depends on injection angle and on the local aspect ratio $\varepsilon = r/R$, as well as on the parameters x and y defined above /25/, it is largest for "passing" particles, that is near the magnetic axis. The opposite is true for the modified electron multiplier F_e provided that Z_b is smaller than Z_{eff}. This means that the combined correction ($F_{nc} \cdot F_e$) is almost constant over a wide range of ε and Z_{eff} /25/. Hence neo-classical effects owing to the toroidal magnetic field configuration need no more a detailed consideration provided that the beam axis lies in the midplane (or equatorial plane) and is directed at a sufficiently grazing angle with respect to the magnetic flux surfaces such that all ions are born into passing orbits (F_{nc} is zero for ions in "blocked" orbits).

By inserting average values of bulk electron density and temperature in eqs.(13) and (14) we can now give an estimate for the current drive efficiency γ (c.f. eq.(1)) in a tokamak configuration:

$$\frac{I_{bd}}{P_{abs}} = \frac{\pi\, a^2 \cdot j_{fi} \cdot F_e \cdot F_{nc}}{\pi\, a^2 \cdot 2\pi \cdot R_o \cdot p_{fi}} = \frac{\gamma}{\bar{n}_e \cdot R_o}$$

Hence:

$$\gamma = \frac{Z_b \cdot e}{\pi \cdot A_b \cdot m_p} \cdot \xi_o \frac{\bar{\tau}_s \cdot \bar{n}_e}{\bar{v}_c} \cdot J(\bar{x},y) \cdot F_e(\bar{\varepsilon}, Z_{eff}) \cdot F_{nc}(\bar{\varepsilon}, \bar{\xi}_o, \bar{x}, y) \qquad (15)$$

By observing the scaling of $\overline{\tau_s}$ (c.f. eq.(9)) and of $\overline{\nu_c}$, γ for neutral beam current drive is found to be independent of density and to increase proportional to $\overline{T_e}$, as has been already mentioned in context to eq.(7a). (F_{nc} depends on injection angle and local aspect ratio, but not on the bulk plasma density and temperature). Therefore eq.(15) can be used for extrapolating γ to reactor parameters. Using relevant numbers and referring to the injection of a D^0-beam with a given direction, eqs.(13), (14) and (15) can be written as:

$$\eta_{fi} = 157 \cdot \left(\frac{10^{14}\,cm^{-3}}{n_e}\right) \cdot T_e \cdot \xi_o \cdot J(x,y) \left[\frac{A/cm^3}{W/cm^3}\right] \qquad (16)$$

$$\gamma = 0{,}25 \cdot \bar{T}_e \cdot \bar{\xi}_o \cdot J(\bar{x},y) \cdot F_e(\bar{\varepsilon},Z_{eff}) \cdot F_{nc}(\bar{\varepsilon},\bar{\xi}_o,\bar{x},y) \; [A/W \cdot m \cdot 10^{20} m^{-3}] \qquad (17)$$

where T_e is in keV. With this equation we have calculated the theoretical efficiency of the DIII-D experiment as shown in the Table /26/.

When solving the kinetic equation for lower hybrid current drive the situation becomes less transparent since there are no newly created high-energy particles to define the source term in velocity space as before in the neutral beam case. Speaking in quite general terms the Landau-damping of waves causes the wave momentum along the magnetic field direction to be transferred to suprathermal electrons which move at about the same speed as the parallel phase velocity of the wave. Thus an electric current is carried by these resonant high-speed electrons because - being relatively collisionless - they retain their parallel momentum longer than the bulk plasma electrons /27/. As the driving wave has a whole spectrum of parallel phase velocities v_{p1} ... v_{p2}, quasilinear Landau damping theory suggests that there is a very strong wave-induced stochastic diffusion inside the corresponding range of electron velocity space. This leads to a flattening of the parallel distribution function until a plateau-like shape is attained within this interval whereas elsewhere the distribution function

remains Maxwellian. The result of a numerical solution to the kinetic equation, which follows this concept, is shown in Fig.1b). The height of the plateau is given by the value of the unperturbed Maxwellian at $w_1 = v_{p1}/v_{te}$ and defines the density of the suprathermal electron population. The basis of this empirical model is the ad-hoc assumption of an anomalously large velocity space diffusion in the resonant region - as mentioned above - but this assumption, ultimately, remains unjustifiable /28/. The existence of a constant value for the electron parallel velocity distribution in the interval $w_1 \ldots w_2$ allows an easy calculation of the current density carried by these suprathermal electrons, as well as of the power density needed to sustain this plateau against collisions with the bulk plasma particles which tend to restore the Maxwellian equilibrium distribution. This power density determines the quasi-linear wave absorption coefficient. The ratio of current density to power density yields the local figure of merit. The two-dimensional distribution function including relativistic effects can be handled by numerical methods only /29/. Their results can be approximated, in the limiting case of a narrow wave spectrum $(v_{p1} - v_{p2}) \to 0$, by the expression:

$$\eta_{fe} = j_{fe}/p_{fe} = \frac{v_p^2}{c^2} \cdot \frac{4}{5+Z_{eff}} \cdot \frac{e}{m_e \cdot \nu_c \cdot c} \cdot f(\Theta, v_p/c, Z_{eff}) \qquad (18)$$

where ν_c is a collision frequency normalized to the speed of light c; f is a weak function of the bulk electron temperature in terms of the electron rest energy, $\Theta = k \cdot T_e/m_{eo} \cdot c^2$ (Θ=1 corresponds to T_e = 511 keV). f(0) is equal to 1 in the non-relativistic limit (Θ=0), thus η_{fe} is proportional to $v_p^2 = v^2_{be}$ up to $v_p/c \tilde{=} 0{,}8$ /30/. In this case η_{fe} grows proportional to E_{be}, as we have already found in our simple model, c.f. eq.(7b). Upon introducing the parallel wave index $N_{\parallel} = c/v_p$, eq.(18) reads in practical units (with $\ln \Lambda_e = 17$):

$$\eta_{fe} = \frac{4635}{N_{\parallel}^2(5+Z_{eff})} \cdot \frac{10^{14}\,cm^{-3}}{n_e} \cdot f(T_e, N_{\parallel}, Z_{eff}) \quad \left[\frac{A/cm^2}{W/cm^3}\right] \qquad (19)$$

which is valid for $N_{\parallel} > 1{,}25$ in the non-relativistic limit. For a rough estimate of the current drive efficiency γ we may set f = 1, and we again

assume (as we did in eq.(15) for neutral beam current drive) that the plasma parameters are constant over the plasma cross-section. Hence

$$\gamma = \bar{n}_{14} \cdot R_o \cdot \frac{I_d}{P_{abs}} = \bar{n}_{14} \cdot R_o \cdot \frac{j_{fe} \cdot \pi a^2}{p_{fe} \cdot \pi a^2 \cdot 2\pi R_o}$$

$$= \frac{7{,}4}{\overline{N_{\parallel}^2} \cdot (5+Z_{eff})} \quad [A/W \cdot 10^{20} m^{-3} \cdot m] \qquad (20)$$

This expression was used to evaluate the theoretically expected γ-values in Refs./3/ and /4/ by taking a suitable average over $(1/N_{\parallel}^2)$ at the location where the wave power is absorbed (as indicated by the horizontal bar in eq.(20)).

In a plasma with finite electron temperatures the simple quadratic relationship between η_{fe} and v_p can only be used when v_p is sufficiently large compared to the electron thermal speed v_{te}. A comparison with numerical simulations shows that this is the case for $w = v_p/v_{te} > 3{,}5$ /31/ and $Z_{eff} = 1 \ldots 2$ /32/ (with $v_{te}^2 = kT_e/m_e$), which is equivalent to $N_{\parallel} < 6{,}5/\sqrt{T_e[keV]}$. Together with $N_{\parallel} > 1{,}25$ these bounds define a range in parameter space which is adequate for our considerations and where eq.(20) applies, for example for electron temperatures up to about 30 keV.

When relativistic effects are taken into account a slight dependence on the plasma electron temperature is found /29/. In simplified terms: the colliding particles become "heavier" at higher energies which makes collisional momentum transfer more difficult, thus prolonging the particle slowing down times. The correction factor f depends on the velocities of suprathermal and bulk plasma electrons, as well as on the number of the bulk plasma electrons (via Z_{eff}). In Figs. 2a) and 2b) we present two examples of such corrections. The normalized figure of merit $\eta(T_e)/\eta(T_e=0)$ is plotted to show the v_p-dependence (or $N_{\parallel}$-dependence) for $Z_{eff} = 1$ in the top figure /33/, and the Z_{eff}-dependence in the limit $v_p \to c$ in the bottom figure /34/. It can be readily seen that this theory predicts a 50 % increase in efficiency for $N_{\parallel} = 1{,}5$ (which corresponds to the maximum power in the PLT-spectrum) when the plasma electron temperature is raised from about zero to 20 keV.

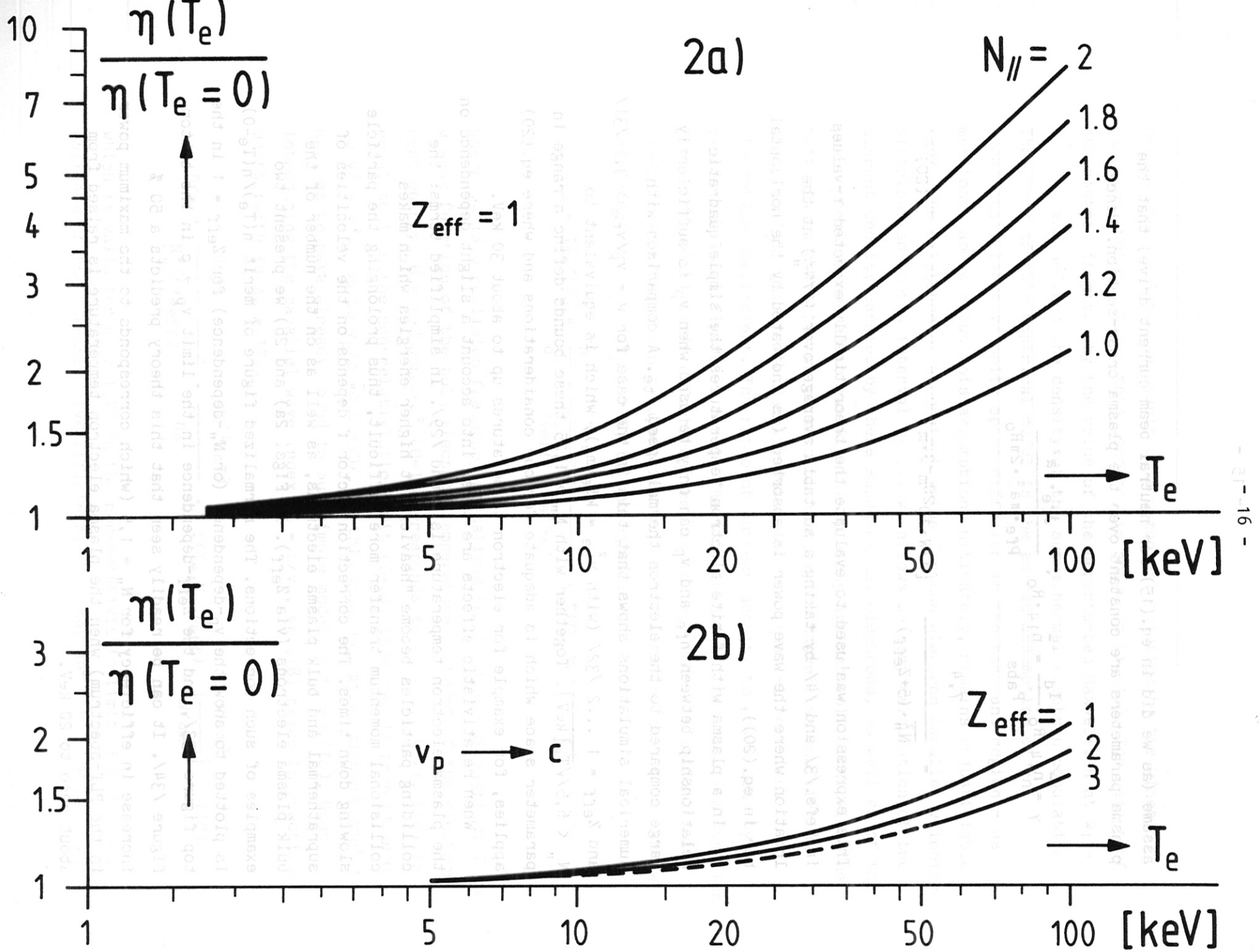
2a)
$\frac{\eta(T_e)}{\eta(T_e=0)}$
$N_{//}$ = 2
1.8
1.6
1.4
1.2
1.0
Z_{eff} = 1
T_e
[keV]
2b)
Z_{eff} = 1
2
3
$v_p \longrightarrow c$

As seen from eq.(18) the parallel phase velocity is the only wave feature which enters into the figure of merit: v_p should be as high as possible. (This trend is somewhat weakened by the slight v_p-dependence of the correction factor $f(\theta)$, see Fig.2a)). But v_p must not surpass a certain limit since faster waves suffer from conversion into a different mode which does not contribute to current drive. Conversely, the parallel refractive index $N_{\parallel}$ in eqs.(19) and (20) has a lower bound, the so-called accessibility limit N_{acc}, which is a function of wave frequency, and of the background plasma properties density and magnetic field strength. Out of a power spectrum $P(N_{\parallel})$ of slow waves launched at the plasma edge only those waves are useful for current drive at a particular location, for which $N_{\parallel} > N_{acc}$. To visualize this constraint we have plotted N_{acc} for a plane DT-plasma in a constant magnetic field (5,5 Tesla) and with two working frequencies, see Fig.3) /35/*). Also indicated is a typical wave power spectrum $P(N_{\parallel})$, with $N_{\parallel} = 1{,}5 \pm 0{,}5$. When the plasma density is raised with wave power kept constant, the driven current is reduced for two reasons: the accessible part of the wave spectrum shrinks owing to the shift of N_{acc} to higher $N_{\parallel}$-values thus reducing the figure of merit (eq.19) and the efficiency (eq.20), in addition the accessible fraction out of the launched wave power decreases. Such a trend was observed in lower hybrid experiments /36/. In the complicated toroidal topology of a tokamak plasma the accessible $N_{\parallel}$-values must be found by numerical calculations ("ray-tracing"). It follows that optimum current drive efficiency requires the wave power to be concentrated in a narrow spectrum which is squeezed towards N_{acc}.

No constraint with regard to $N_{\parallel}$ exists for fast waves /5/ which have been advertised, therefore, for wave-induced current drive at the centre of dense plasmas /32,37/. But up to now no conclusive evidence for current drive with this wave has been reported, even if direct wave-electron interaction could be observed /38/.

---

*) at higher generator frequencies the N_{acc} vs. n_e-dependence does not change any more /35/.

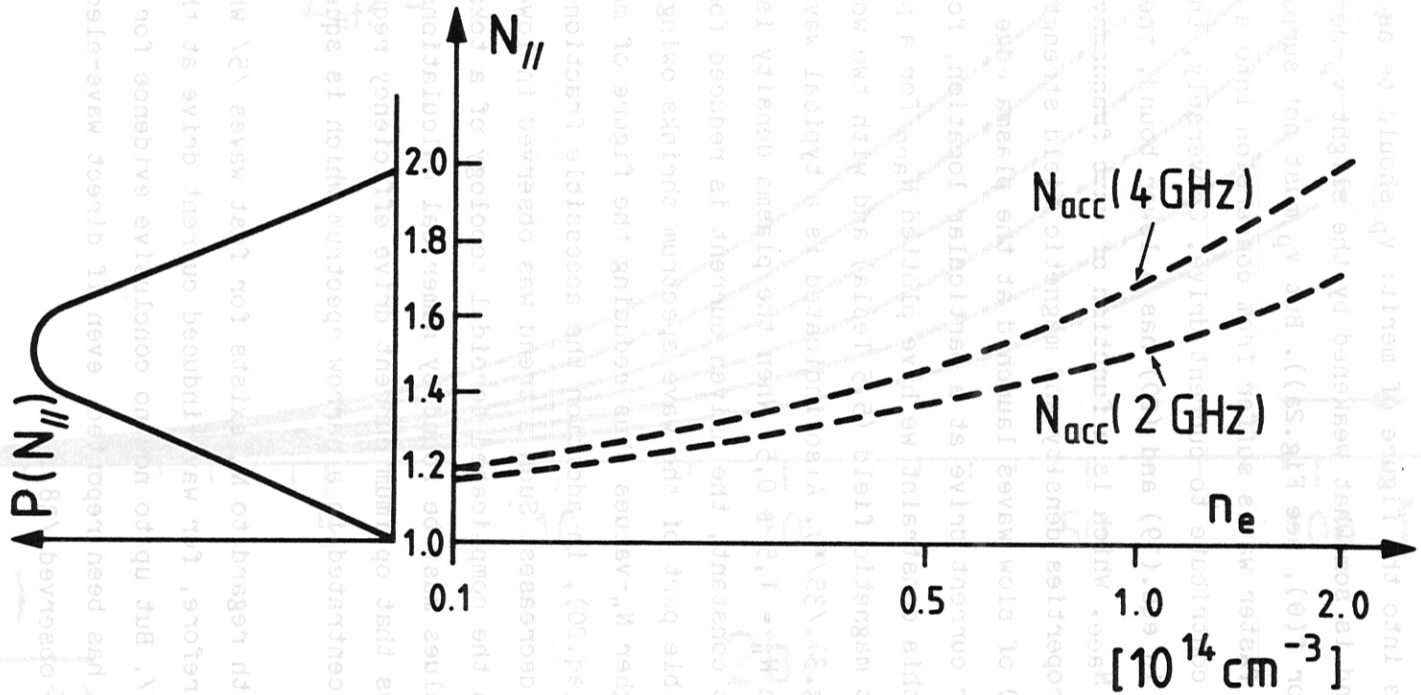

Fig.3): The accessibility limit N_{acc} in a plane DT-plasma is plotted versus electron density for two generator frequencies (from Ref./31/). Out of a wave power spectrum $P(N_{\parallel})$ only waves with parallel refractive indices $N_{\parallel}$ larger than N_{acc} can pentetrate through the plasma from the outer edge up to a point charaterised by the density n_e

The dependence on plasma cleanliness, as expressed by the Z_{eff}-number, is an explicit one for lower hybrid current drive, c.f. eq.(20). In the case of neutral beam driven current, the Z_{eff}-value enters via the electron back current, c.f. eq.(14), but it has the opposite trend: the net current increases with the Z_{eff}-number in a way which depends on beam characteristics (Z_b) and on the toroidal topology.

Let us now compare the two locally variable quantities η_{fi} and η_{fe}, c.f. eqs.(16) and (19). Their ratio depends on the bulk electron temperature, on the Z_{eff}-value, and - though in an indirect way - on the plasma density via the condition $N_{\parallel} > N_{acc}$ (n_e), as illustrated in Fig.3). The other multipliers like initial pitch angle ξ_o, deposition factor J_o, etc., remain within rather narrow margins for any plausible set of beam-plasma parameters. As an example let us choose $Z_{eff} = 2$, $\xi_o = 0{,}8$ which defines $J = 0{,}18$, and $F_e \cdot F_{nc} = 0{,}5 \ldots 0{,}6$ for all ε-values of interest /39/; furthermore we shall consider $N_{\parallel} = 1{,}7$ which is well above the limiting number 1,25 introduced on p.14 and sets the accessibility limit at about $n_e = 1 \cdot 10^{14}$ cm^{-3} for frequencies $\geq$ 4 GHz*). We find that η_{fi} is bigger than η_{fe} when T_e is above 18,4 keV. But this transition temperature depends strongly on the $N_{\parallel}$-value chosen, that is on the velocity of the resonant electrons whose accessibility limit decreases when the density gets higher.

---

*) higher frequencies are to be preferred in order to avoid wave damping by fuel ions and α-particles /35/.

V. Extrapolation to Reactor Conditions

Proceeding from present current drive experiments, as listed in the Table on page 6, towards reactor conditions comprises a number of foreseeable changes:

- electron densities and temperatures, as well as the toroidal plasma current, must be increased by more than an order of magnitude,
- plasma dimensions will become larger by a factor 2 ... 4 in linear scale with the shape of the toroidal plasma - and hence the relevant numbers for the aspect ratios - remaining nearly the same,
- the magnetic confining field strength is higher by a factor of about 2,
- the plasma effective charge Z_{eff} must be lowered to values slightly above unity which means a reduction by factors up to 5 compared to what is encountered in today's current drive experiments.

These are, indeed, major increases in background plasma density and temperature which must be accomplished, and we have to rely on theory when speculating about current drive under these completely new plasma conditions.

In doing so we shall follow the route already indicated previously by considering the local steady-state relationship between the non-inductive current density j_f of suprathermal particles which flow along the magnetic field lines inside the toroidal-shell volume between two nested flux surfaces, and the density of power p_f which is deposited in this volume element from the driver via interactions with the bulk plasma particles:

$$j_f = \eta_f \cdot p_f \qquad (21)$$

Here η_f is the local figure of merit whose dependence on the background plasma properties has been discussed in the preceding Chapter IV with the following results:

1) In lower hybrid current drive the product ($\eta_{fe} \cdot n_e$) has no direct relationship with bulk electron density n_e and temperature T_e. Accessibility constraints and relativistic effects modify the useful power spectrum and its figure of merit, both work in opposite directions when n_e and T_e are raised thus tending to cancel each other. In short, we expect only minor changes in ($\eta_{fe} \cdot n_e$) on the way towards reactor conditions, for example a modest increase owing to a reduction in Z_{eff}.
2) For neutral beam current drive the product ($\eta_{fi} \cdot n_e$) grows proportional to T_e.

It follows that the power drawn from a driver and absorbed by a high-density high-temperature plasma can be more efficiently converted into toroidal plasma current with neutral beam injection than with lower hybrid waves, which is of particular concern for the central plasma regions.

Let us now discuss in some detail how this power absorption - or rather the power density p_f in eq.(21) which has to sustain the driven current in steady state - varies with bulk plasma parameters. The neutral particle beam, on passing through the bulk plasma, is attenuated by ionizing and charge-exchanging collisions between beam and plasma particles. Hence the deposited power is simply given by the ionization rate times the energy carried by each (of the monoenergetic) beam particle(s). It turns out that ionization by impact on the background ions is the dominant process over the whole of the energy range of interest, and - since the beam particle speed is much higher than the bulk ion velocities - the ionic cross-sections depend on beam energy only but not on plasma temperature. Hence all plasma ions participate in beam attenuation, and the fast ion production rate S_o (c.f. eq.(11)) is found to be proportional to n_i/E_{bi}^{α} (with $\alpha = 0.82$) /40/. This scaling suggests that the deposited power density can be controlled by adjusting n_i and E_{bi}. In particular, the amount of beam power which traverses the plasma without being absorbed ("shine-through") must be kept within acceptable limits /41/.

With lower hybrid current drive the situation is quite different since wave absorption and subesequent power deposition occurs via Landau damping at a selected number of resonant electrons. They are those electrons out of

the bulk distribution which move at about the same speed as the parallel phase velocity v_p of the wave. Their number varies exponentially with $w^2 = (v_p/v_{te})^2$. Hence wave power deposition depends strongly on electron temperature: it increases rapidly when the electron temperature is raised. Strong quasi-linear wave damping is expected when $w = v_p/v_{te} < 2{,}8...4{,}2$ /42/, say for $w < 3{,}5$ (with $v_{te}^2 = T_e/m_e$). Expressing the latter number value as a condition to the parallel refractive index $N_\parallel$ of the lower hybrid wave, one finds that strong absorption occurs when:

$$N_\parallel > N_{eld} = \frac{6{,}4}{\sqrt{T_e}} \qquad (22)$$

with T_e in keV. Here we have introduced N_{eld} to characterise the ratio between phase velocity and electron thermal velocity where strong Landau damping takes place according to quasi-linear theory /43/. Incidentally, the value $w = 3{,}5$ which is characteristic for the transition between free propagation and strong absorption of slow waves, equals the lower bound on w introduced on p.15: η_{fe} is proportional to v_p^2 for $w > 3{,}5$.

It is quite obvious that ineq.(22) puts a constraint on lower hybrid wave propagation in a given high-temperature plasma which is quite analogous to the lower barrier on $N_\parallel$ caused by in-accessibility to a high-density plasma, as discussed in Chapter IV. Thus lower hybrid slow waves with a given frequency can only propagate freely through a plasma in a given magnetic confining field when their wave power spectrum $P(N_\parallel)$ lies within the bounds:

$$N_{eld}(T_e) > N_\parallel > N_{acc}(n_e) \qquad (23)$$

As the slow waves are launched with a given $N_\parallel$-spectrum at the plasma periphery and propagate from there into regions of increasing plasma density and temperature, they can either penetrate to the plasma centre or they are absorbed at some outer radial position. In a plane plasma the two possibilities are drawn schematically in Fig.4) for the case of low (T_{01}) and high (T_{02}) central temperature. In the latter case wave power deposition is shifted away from the centre. The driven current generates an off-axis peaking in the radial current density distribution (which can cause an MHD-unstable situation). As non-inductive current drive requires

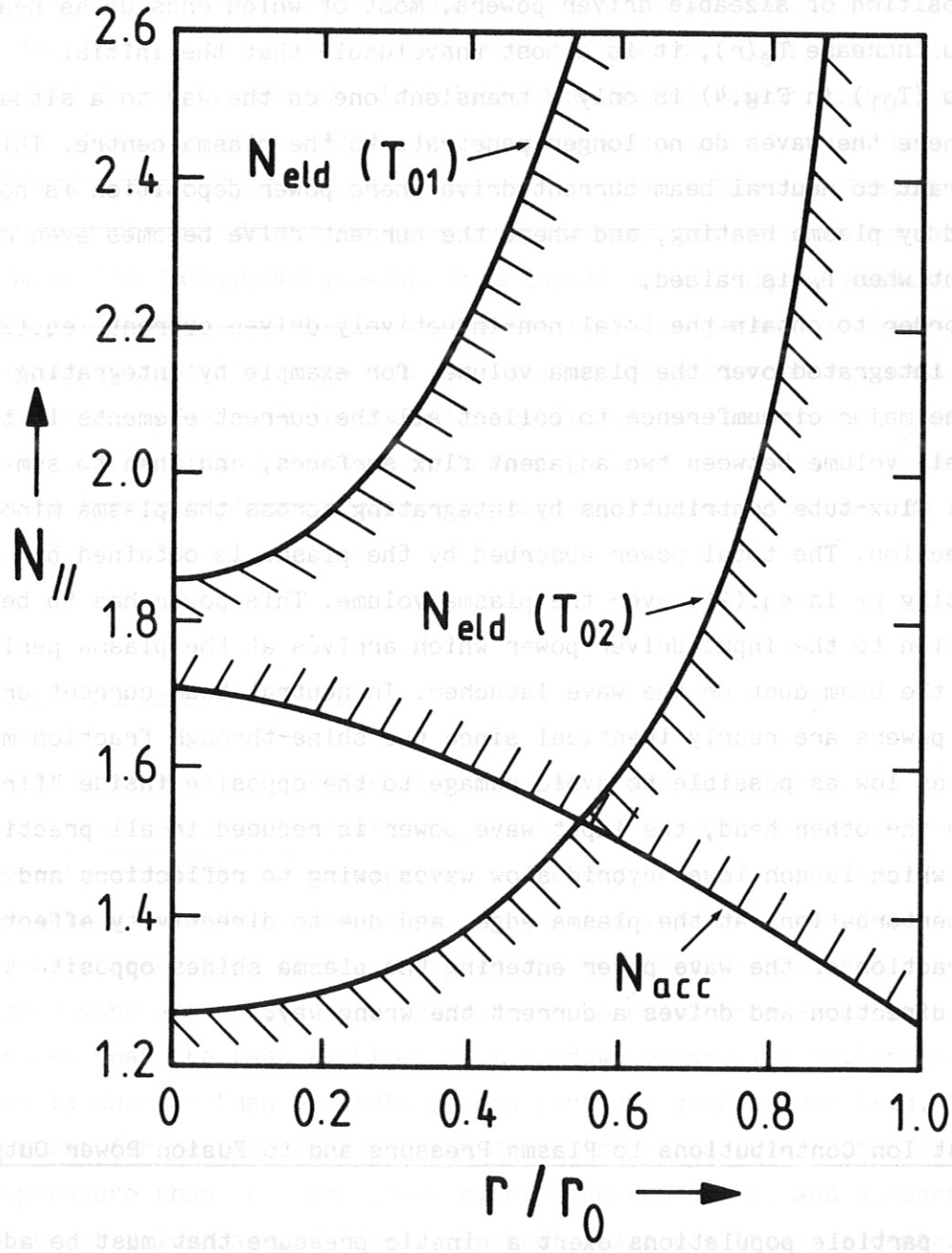

Fig.4): Radial dependence of N_{eld} and N_{acc} for given profiles of electron density and temperature with two peak values $T_{01} < T_{02}$ (schematically). Lower hybrid waves can only penetrate from the outside when their $N_{//}$-values lie inside the regions indicated by hatchings (extended version of Fig. 1 in Ref. /42 /). Current drive is most effecient when $N_{//}$ is minimum, but $N_{//}$ has N_{acc} as lower bound.

the deposition of sizeable driver powers, most of which ends up as heating power to increase $T_e(r)$, it is almost unavoidable that the initial scenario (T_{01}) in Fig.4) is only a transient one on the way to a situation (T_{02}) where the waves do no longer penetrate to the plasma centre. This is in contrast to neutral beam current drive where power deposition is not hampered by plasma heating, and where the current drive becomes even more efficient when T_e is raised.

In order to obtain the total non-inductively driven current, eq.(21) must be integrated over the plasma volume, for example by integrating first along the major circumference to collect all the current elements in the same shell volume between two adjacent flux surfaces, and then to sum up over all flux-tube contributions by integrating across the plasma minor cross-section. The total power absorbed by the plasma is obtained by integrating p_f in eq.(21) over the plasma volume. This power has to be set in relation to the input driver power which arrives at the plasma periphery through the beam duct or the wave launcher. In neutral beam current drive the two powers are nearly identical since the shine-through fraction must be kept as low as possible to avoid damage to the opposite inside "first" wall. On the other hand, the input wave power is reduced in all practical systems which launch lower hybrid slow waves owing to reflections and non-linear perturbations at the plasma edge, and due to directivity effects: a small fraction of the wave power entering the plasma shines opposite to the desired direction and drives a current the wrong way.

VI. Fast Ion Contributions to Plasma Pressure and to Fusion Power Output

The fast particle populations exert a kinetic pressure that must be added to the isotropic pressure of the bulk plasma which is in thermal equilibrium. Depending on fast particle characteristics and on bulk plasma properties, this additional pressure can become of importance - especially when the plasma is operated near the critical pressure that can be supported by the magnetic confining field of a tokamak (the "beta-limit"). For typical current drive scenarios the pressure contribution from the hot electron population is smaller by more than an order of magnitude than that of the hot deuterium ions, and can be neglected therefore.

In order to accomodate the kinetic pressure of a beam-fuelled suprathermal deuterium ion population it is conceivable that the pressure of the thermal background plasma must be lowered. This reduction of the product $(n_i \cdot T_i)$, however, diminishes the thermonuclear fusion power output of the bulk DT-plasma. Thus, one could ask the question how the reduced thermal fusion power output compares with the additional fusion rates from the suprathermal deuterium ions reacting with the tritium and deuterium ions of the background plasma. This question can only be answered for specific beam/plasma systems where the relevant parameters have been quantified. For the so-called NET-IIIA configuration an evaluation has been carried out /44/ with the result that in the low-temperature cases ($\bar{T}$ = 10 keV) the fusion power output from beam-induced reactions exceeds the losses due to the bulk plasma pressure reduction. The opposite is true for the high-temperature scenarios ($\bar{T}$ = 20 keV).

VII. Summary and Conclusion

Non-inductive current drive with neutral beams and with lower hybrid slow waves have been compared with regard to their performances observed at present, and those to be expected in future tokamak reactors. This comparison is made by investigating how the local figure of merit and the specific absorption of driver power are modified when plasma density and temperature are raised from present-day to reactor-relevant values. It is assumed that the fast particle slowing-down occurs via collisions in a time that is shorter than the bulk plasma particle confinement time. The figure of merit for neutral beam current drive increases much faster with electron temperature than that for lower hybrid current drive, and surpasses the latter at values around 20 keV. Neutral beams can traverse dense plasmas provided that the beam particle energy is high enough. This is in contrast to lower hybrid slow waves which do not all penetrate into dense and hot plasmas because of mode conversion and absorption effects. This limits

their applicability to the outer plasma regions - in particular when the central plasma has been heated by driver power deposition. A more precise judgement can only be made after applying both drivers to given plasma configurations. Yet theory predicts that the global current drive efficiency γ for lower hybrid waves will become only slightly better than the values seen in present large experiments with their $N_{\parallel}$-spectrum tailored for optimum current drive. For neutral beam current drive in hot plasmas one expects γ-values of 0.3 to 0.4 /44/. This means that the two efficiency numbers should come quite close to each other whereas nowadays they are apart by roughly an order of magnitude.

The pressure-driven bootstrap current has not been considered in the present Report. It can significantly enhance the non-inductively generated current when the driven power deposition is properly shaped /45/.

VIII. References

/1/ T.C. Simonen et al., Phys.Rev.Letts. 61 (1988) 1720. G.D. Porter et al., Proc. 16th EPS Conf. Contr. Fusion and Plasma Phys., Venice (1989), Part IV, p. 1251

/2/ K. Ushigusa et al., Nucl. Fus. 29 (1989) 1052. See Fig. 1 in particular.

/3/ J.E. Stevens et al., Nucl. Fus. 28 (1988) 217

/4/ F. Leuterer et al., Proc. 8th AIP Conf. Radio Freq. Power in Plasmas, Irvine, CA (1989), p. 95. Annual Report 1989, IPP Garching, p. 53. (Note that here the efficiency is defined with $\bar{n}_e$ in units of 10^{13} cm^{-3}).

/5/ Slow waves have their oscillating E-field vector directed along the magnetic confining field lines, fast waves perpendicular to this direction.

/6/ N.J. Fisch, Revs. Mod. Phys. 59 (1987) 175.

/7/ D.R. Mikkelsen, C.E. Singer, Nucl. Technology/Fusion 4 (1983) 237

/8/ J.G. Cordey, Chapter 6, p. 333, in "Applied Atomic Collision Physics", Vol. 2 "Plasmas", Academic Press Inc. (1984)

/9/ t_{se} can be evaluated with the help of eq. 4.39 on p. 92 in "Plasma Physics for Nuclear Fusion" by K. Miyamoto. MIT Press (1980).

/10/ eqs.(4) and (5) of Ref. /7/.

/11/ Dr.K. Ushigusa. Private Communication.

/12/ this was done with the help of eq.(20) in Chapter IV of this Report which is the corrected version of eq.(2) in Ref./3/.

/13/ S.C. Luckhardt, Nucl. Fus. 27 (1987) 1914.

/14/ J.M. Rax, D. Moreau. Nucl. Fus. 29 (1989) 1751.

/15/ F. Leuterer, private communication.

/16/ K. Ushigusa et al., Proc. 12th IAEA Conf. Plasma Phys. Contr. Nucl. Fus. Res., Nice (1989), Vol. 1, p. 621

/17/ See Fig. 4b) of Ref./16/.

/18/ J.G. Cordey et al., Nucl. Fus 15 (1975) 441.

/19/ R.J. Goldston, Nucl. Fus. 15 (1975) 651.

/20/ J.G. Cordey, Proc. 5th IAEA Conf. Plasma Phys. Contr. Nucl. Fus. Res., Tokyo (1974), Vol. 1, p. 623.

/21/ W.W. Heidbrink, General Atomics Report A-19709 (August 1989).

/22/ S. von Goeler et al., Nucl. Fus. 25 (1985) 1515
J. Stevens et al., Nucl. Fus. 25 (1985) 1529.

/23/ See Fig. 22 in K. Uehara, T. Nagashima, Proc. 3rd Joint Varenna-Grenoble Symp. EUR 7979 EN (1982) 500.

/24/ eq.(9) of Ref/7/.

/25/ K. Okano, Nucl. Fus. 30 (1990) 423.

/26/ Υ is independent of A_b so we can apply it to the H^0-Injection into He-plasmas of DIII-D for which we took $Z_{eff} = 2$, $\xi_o \cong R_{tang}/R_o$, $F_{nc} = 1$, and F_e at ro/2.

/27/ N.J. Fisch, Phys. Rev. Letts. 41 (1978) 873.

/28/ See text on p. 188 of Ref./6/.

/29/ C.F.F. Karney and N.J. Fisch, Phys. Fluids 28 (1985) 116

/30/ see Fig. 20 of Ref./6/

/31/ G. Tonon in J. M. Ané et al., Report EUR-CEA-FC-1380 (October 1989), in particular Fig. II.2.2.)

/32/ D.A. Ehst and K. Evans, Jr., Nucl. Fusion 27 (1987) 1267, in particular Fig.3

/33/ from Fig. 3 of Ref./29/.

/34/ Table II of Ref./29/.

/35/ Ref./31/, in particular Fig.II.2.3.

/36/ (see Fig.(7a) of Ref./3/.

/37/ D.A. Ehst, Report ANL/FPP/TM 219 (March 1988) Argonne National Laboratory.

/38/ Y. Uesugi et al., Proc. 16th EPS Conf. Control. Fusion Plasma Phys., Venice (1989), Vol. 13B., Part IV, p. 1259.
L.-G.Ericksson, T.Hellsten, Nucl. Fus. 29 (1989) 875.

/39/ See Fig. 2 of Ref./25/.

/40/ M. Cox et al., Final Report to NET-Contract 85/089/PH (1987) (unpublished).

/41/ The beam energies involved are in the range of several hundreds of kilovolts per nucleon which is about an order of magnitude higher than the energy in present injection experiments. The development of such new injection systems is now under way, and the variability of the beam energy E_b is taken into serious consideration.

/42/ P.T. Bonoli, M. Porkulab, Nucl. Fusion 27 (1987) 1341. Note that these authors use the definition $v_{te}^2 = 2\ kT_e/m_e$.

/43/ M. Brambilla in "Physics of Plasmas Close to Thermonuclear Conditions". Proc. Course Varenna (1979). EUR FU BRU/XII/476/80. Vol. 1, p. 298.

/44/ D. Eckhartt, Final Report to NET Contract 268/87-6(1989) (unpublished).

/45/ D.A. Ehst et al., Phys.Rev.Letts. 64 (1990) 1891).